

NSM FRP shear contribution in the strengthened RC beams

Renata Kotynia

Technical University of Lodz, Lodz, Poland

ABSTRACT: The existing research and engineering practice on RC beams shear strengthened with near surface mounted (NSM) fiber reinforced polymer (FRP) materials are extremely limited. However, the first results have been very promising and aroused interest of the worldwide FRP community. Based on the three published approaches the paper shows comparable analysis of calculated and experimental results of the NSM shear contribution. The most versatile model by Bianco et. al considers two main failure mechanisms: FRP debonding and the concrete tensile fracture approach. However, it overestimates the semi-cone surface of the fracture plane.

1 INTRODUCTION

The shear strength of reinforced concrete (RC) beams can be successfully increased by gluing the fiber reinforced polymers (FRPs) into thin slits cut onto the concrete cover on the lateral sides of the beams. Higher bond area between the FRP stirrups and concrete than that in the externally bonded (EB) technique provides higher bond stress transferred by the NSM reinforcement. Compared to externally bonded FRP strips, the NSM technique benefits in reducing of the amount of installation work, protecting against fire, mechanical damage, accidental impact, and not changing the aesthetic of the structure. The research on the shear strengthened RC beams with the NSM FRP started a few years ago, thus the number of experimental tests and practical applications of this technique are rather limited.

Existing standards for the shear strengthening of RC members with FRPs consider mainly the externally bonded techniques. The design shear resistance of strengthened RC members is proposed by the *fib* Bulletin (2001) as a sum of three components: concrete $V_{Rd,c}$, transverse steel reinforcement $V_{Rd,s}$ and the FRP shear reinforcement contribution $V_{Rd,f}$.

$$V_{Rd} = V_{Rd,c} + V_{Rd,s} + V_{Rd,f} \quad (1)$$

where: $V_{Rd,c}$, and $V_{Rd,s}$ to be calculated in accordance to the current building guidelines for the RC structures. The contribution of the composite stirrups to the shear strength has been proposed by the following four approaches: adapted *fib* (2001), De Lorenzis (2002), Nanni et. al (2004) and Bianco et. al (2009). The first one defines the share of FRP reinforcement in the shear strength similar to the transverse steel reinforcement. Two second empirical proposals derived from the formulation by De Lorenzis (2002), define the FRP contribution based on the FRP to concrete bond condition along the effective bond length of the NSM FRP stirrup cut by a diagonal shear crack. The third model by Bianco et. al. (2009) underlines the occurrence of the particular failure mode effected by the detachment of the concrete cover from the beam core named semi-conical tensile concrete fracture of concrete surrounding each FRP stirrup.

The aim of the paper is to propose easy design recommendation formula for prediction of the NSM shear contribution. Based on the published three approaches by *fib* (2001), Nanni et. al

(2004) and Bianco et. al (2009), the author shows comparable analysis of calculated and experimental results of the NSM shear contribution.

1.1 The fib approach

The NSM FRP contribution value adapted from the *fib* Bulletin (2001) assumes, that the composite stirrups crossed by a shear crack transmit the transversal force expressed by the following formula.

$$V_f = \frac{A_f \varepsilon_{f,b} E_f}{s_f} z (\cot \theta + \cot \alpha) \sin \alpha \quad (2)$$

$$A_f = w_f t_f \quad (\text{for FRP strips}); \quad A_f = \frac{\pi d_f^2}{4} \quad (\text{for FRP bars}) \quad (3)$$

where: s_f – spacing between the FRP reinforcement along the longitudinal beam's axis; $\varepsilon_{f,b}$ – ultimate FRP bond strain; A_f - cross-section area of the one arm of the FRP reinforcement; E_f – elasticity modulus of the FRP reinforcement; α_f – inclination of the FRP reinforcement to the beam's axis; θ – inclination of the critical shear crack to the beam's axis; z – arm of the internal forces; $z=0,9d$; w_f , t_f – width and thickness of the FRP strip's cross-section; d_f – diameter of the FRP round bar's cross-section.

Based on the published test results of the NSM FRP shear strengthened beams, the author assumed the FRP contribution to the shear strength the ultimate bond FRP strain of 0.004 for the strips and 0.002 for the round bars.

1.2 Modified Nanni et. al model

The second model, proposed by Nanni et. al (2004) derived from the pioneer formulation by De Lorenzis (2002), defined the FRP contribution to the shear capacity based on the assumption that the group of the strips cut by the critical diagonal shear crack, transfer the lateral forces involved, only those that meet the conditions for anchoring in concrete after both sides of the cracks. It means that to avoid FRP debonding, the limit of the shear stress between NSM and concrete should be resisted by the FRP stirrup. Depending on the shape of the cross-section FRP reinforcement, the shear capacity determine the formulas (4a) and (4b) for the strips and bars, respectively.

$$V_f = 4(w_f + t_f) \tau_b L_{tot} \sin \alpha \quad (\text{for FRP strips}) \quad (4a)$$

$$V_f = 2\pi d_f \tau_b L_{tot} \sin \alpha \quad (\text{for FRP bars}) \quad (4b)$$

where:

τ_b – the average bond strength; L_{tot} – the minimum possible total FRP length expressed by the

sum of the effective bond length of each laminate, determined by $L_{tot} = \sum_i^{n_f} L_i$.

The critical shear crack crossing the total number of the FRP stirrups n_f expressed by (9), divides each i -th laminate into two parts with the values of the shorter part $L_{b,i}$ and the longer part $L_{a,i}$, situated above and below the crack, respectively (see Fig. 1). The conservative Nanni et. al model introduces the NSM FRP bond length reduction by subtracting concrete cover thickness c_{s1} of the NSM stirrup to L_{net} (7). Depending on the mutual position of the shear crack and the NSM FRP reinforcement (see Fig. 2), the minimal $n_{f,min}$ and maximal $n_{f,max}$ number of FRP bars crossed by the shear crack are defined by (6).

The author proposed some modifications to the original Nanni et. al model introducing the inclination both of the NSM FRP and of the critical shear crack to the beam's axis.

To meet the resisting contribution by concrete aggregate interlock, a value of the effective bond length of each FRP stirrup should be limited by maximal value of the embedment FRP length L_{max} expressed by (8). Based on the experimental bond tests two NSM FRP to concrete bond conditions have been proposed: $\varepsilon_{f,b} = 0,004$, $\tau_b = 6,81$ MPa - by De Lorenzis (2002) and $\varepsilon_{f,b} = 0,0059$, $\tau_b = 16,1$ MPa - by Barros & Dias (2005).

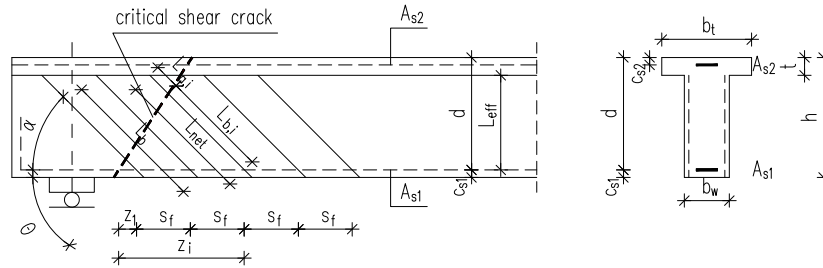


Figure 1. Scheme of calculated anchored length of the NSM stirrup crossed by the diagonal shear crack.

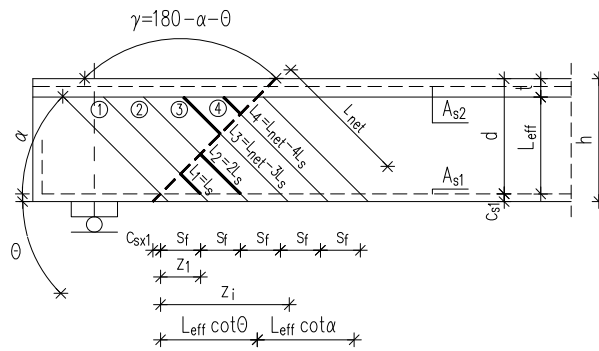


Figure 2. Calculated minimal total effective bond length of the NSM FRP crossed by the shear crack.

$$z_i = z_1 + (n_f - 1)s_f \leq L_{eff} (\cot \theta + \cot \alpha) \quad (5)$$

$$n_{f,min} = \frac{L_{eff} (\cot \theta + \cot \alpha)}{s_f}; \quad n_{f,max} = \frac{L_{eff} (\cot \theta + \cot \alpha)}{s_f} + 1 \quad (6)$$

$$L_b = \frac{h - t}{\sin \alpha}; \quad L_{net} = L_b \sin \alpha - c_{s1} \quad (7)$$

$$L_{max} = \varepsilon_{f,b} \frac{w_f \cdot t_f}{2(w_f + t_f)} \frac{E_f}{\tau_b} \quad (\text{for strips}); \quad L_{max} = \varepsilon_{f,b} \frac{d_f}{4} \frac{E_f}{\tau_b} \quad (\text{for round bars}) \quad (8)$$

$$\begin{cases} L_{b,i} = L_s i \leq L_{max} & i = 1 \dots \frac{n_f}{2} \\ L_{a,i} = L_{net} - L_s i \leq L_{max} & i = \frac{n_f}{2} + 1 \dots n_f \end{cases} \quad (9)$$

$$L_s = \frac{s_f \sin \theta}{\sin(\alpha + \theta)} \quad (10)$$

1.3 Modified Bianco et. al model

The model proposed by Bianco et. al (2009) defined the NSM FRP contribution to the shear capacity based assumption that only those FRP strips transfer the lateral forces, which meet the conditions for anchoring in concrete. The critical shear crack crossing the total number of the FRP stirrups n_f expressed by (6), divides each i -th laminate into two parts with the values of the shorter part $L_{b,i}$ and longer $L_{a,i}$, situated above and below the crack (Fig. 1).

The FRP contribution to the shear capacity in this approach based on the following three experimentally justified failure modes of the strips cut by the critical shear crack: FRP debonding, FRP tensile rupture and concrete semi-conical tensile fracture. The FRP debonding is adapted to define the loss of bond within the adhesive layer, or just a few millimeters inside the surrounding concrete. The tensile fracture of concrete surrounding each NSM strip is characterized by a cone-shaped spalling of the concrete surrounding the embedded FRP length propagating towards the surface of the concrete cover. This failure mode occurs when the surrounding concrete principal stresses exceed the tensile concrete strength (see Fig. 3).

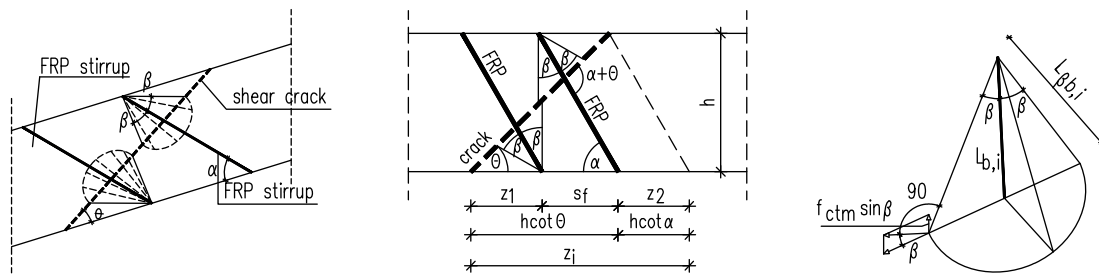


Figure 3. Semi-cone concrete fracture surrounding the NSM FRP stirrup cut by the shear crack.

Based on the existing test results of the RC beams NSM FRP strengthened in shear indicating the most often failure mode due to concrete semi-conical tensile fracture, the author considers this failure mode in the calculated analysis. The maximum NSM FRP contribution on both sides of the beam to its shear strength has been proposed by Bianco et. al (2009) according to the following equation:

$$V_f = \pi f_{ctm} \sin \alpha_f \sum_i^{n_f} L_i^2 \tan^2 \beta_i \quad (11)$$

Where: β_i - the angle between the generatrix of a semi-cone and the axis of the i -th FRP stirrup; L_i - the minimum possible FRP bond length determined by (9), assuming that $L_{net} = L_b = (h-t)/\sin \alpha_f$; f_{ctm} - the average tensile concrete strength perpendicular to the semi-conical surface (Fig. 3), expressed according to EC2 as follows $f_{ctm} = 0,3f_c^{2/3}$, where f_c is the cylinder compressive concrete strength.

The angle β_i is effected by the FRP bond length L_i and has been proposed by Bianco et. al (2006) on the basis of the test bond results as follows:

$$\beta_i = \begin{cases} 32.21 & L_i \leq 30\text{mm} \\ 33.973 - 0.0587L_i & 30\text{mm} < L_i \leq 150\text{mm} \\ 25.17 & L_i > 150\text{mm} \end{cases} \quad (13)$$

Depending on the mutual inclination of the critical shear crack θ and the NSM FRP stirrup α to the beam's axis, the author proposes to use the real FRP bond length as an average height of the minimal and maximal semi-cone crossing the diagonal shear crack in points A and B,

respectively (see Fig. 4). For different values of the angle θ , the average semi-cone surface differs as it is shown in Fig. 4a-c, getting the highest value for the vertical FRP strips.

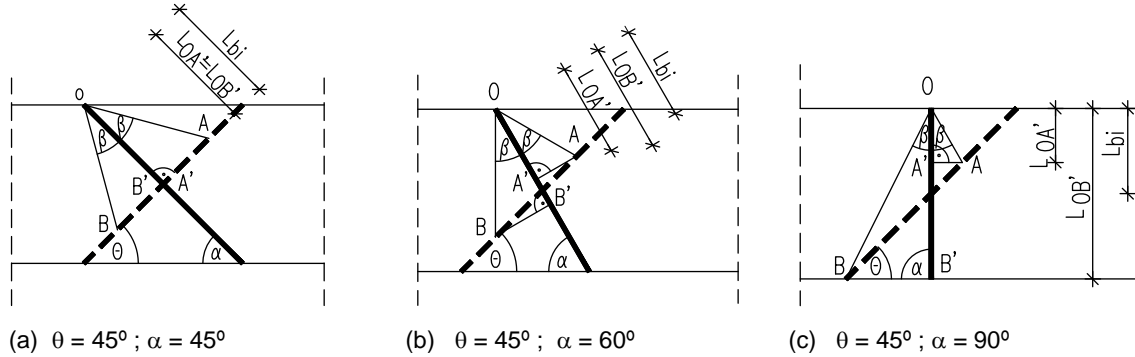


Figure 4. Reduction of the concrete semi-cone surface according to the angles θ and α .

The minimum $L_{OA'}$, the maximum $L_{OB'}$ and the average $L_{avb,i}$ NSM bond length can be calculated according to the following formulas:

$$L_{OA'} = L_{bi} \sin(\alpha + \theta) \cos \beta \sin(\alpha + \theta - \beta) \quad (14)$$

$$L_{OB'} = L_{bi} \sin(\alpha + \theta) \cos \beta \sin(\alpha + \theta + \beta) \quad (15)$$

$$L_{avb,i} = 0,5 L_{bi} \sin(\alpha + \theta) \cos \beta \left(\frac{1}{\sin(\alpha + \theta + \beta)} + \frac{1}{\sin(\alpha + \theta - \beta)} \right) \quad (16)$$

2 ANALYSIS

Three described in the previous section calculated methods of the NSM FRP contribution to the shear capacity of the strengthened RC beams were applied to predict the NSM contribution of several T-section beams tested by De Lorenzis & Nanni (2001), Dias & Barros (2008), Dias et al (2007), Dias & Barros (2010), Kotynia (2007). The beams considered in the analysis were characterised by the average concrete strength varied from above 29,0 MPa to almost 42 MPa and the steel longitudinal reinforcement ratio varied from 2,38% to 2,92%. The transversal steel reinforcement mostly consisted of two-arm stirrups of 6mm and 9,5mm diameter at the various spacing ranged from 180 mm to 300 mm. Some of the collected beams did not have any transversal steel reinforcement. Four types of the CFRP strips differed in dimensions (thickness: 1,4mm, 2mm and 2,4mm; width: 10mm, 16mm and 15mm) and elastic modulus ranged from 105 GPa to 227 GPa, were applied. The groove width was commonly 3mm higher than the FRP strip's thickness (to allow almost 1,5mm side clearance between FRP and concrete) and 2mm deeper than the FRP width. For embedded NSM round bars the grooves had square cross-section with the dimension almost 1,5 to 2 times higher than the nominal FRP diameter. The single span beams were strengthened in the support region for shear with the NSM CFRP strips/bars applied at three angles of 45° , 60° and 90° to the beam axis at the spacing s_f varied from 100 mm to 360 mm. The inclination of the critical shear crack to the beam axis θ was assumed 45° .

The comparison of the test and calculated values of the NSM shear contribution ratio are shown for the minimal and maximal total bond length in Table 1 and Table 2 for the beams strengthened with CFRP strips and round bars, respectively.

Table 1. Comparison of the test and calculated NSM FRP shear strip contribution ratios

Beam	$V_{f,test} / V_{f,cal}$						
	<i>Adapted fib</i>	Modified Nanni et. al (2004)		Modified Bianco et. al (2009)			
	$\varepsilon_f=4,0\text{‰}$	$\varepsilon_f=5,9\text{‰}; \tau_b=16,1\text{MPa}$	$\varepsilon_f=4,0\text{‰}; \tau_b=6,81\text{MPa}$	min L_{tot}	max L_{tot}		
		min L_{tot}	max L_{tot}	min L_{tot}	max L_{tot}		
BI-2/3B ¹	0,98	0,61	0,25	1,44	0,60	1,05	0,47
BI-3/5A ¹	0,97	0,52	0,52	1,22	1,22	1,30	1,30
2S-5LV ²	0,67	0,36	0,21	0,85	0,51	0,35	0,29
2S-8LV ²	0,81	0,31	0,22	0,74	0,52	0,22	0,26
2S-5LI45 ²	1,08	0,39	0,39	0,91	0,91	0,71	0,71
2S-8LI45 ²	0,66	0,21	0,21	0,51	0,51	0,39	0,39
2S-3LI60 ²	1,41	0,96	0,23	2,28	0,55	0,73	0,21
2S-5LI60 ²	1,10	0,48	0,48	1,12	1,12	0,52	0,52
2S-7LI60 ²	0,93	0,44	0,28	1,05	0,67	0,44	0,30
2S-7LV ³	0,53	0,15	0,15	0,36	0,36	0,41	0,41
2S-4LI45 ³	1,09	0,34	0,34	0,79	0,79	0,82	0,82
2S-7LI45 ³	0,88	0,49	0,28	1,15	0,66	0,69	0,61
2S-4LI60 ³	0,97	0,42	0,29	1,00	0,69	0,88	0,80
2S-6LI60 ³	0,84	0,57	0,57	1,34	1,34	1,04	1,04
4S-4LI45 ³	0,84	0,26	0,26	0,61	0,26	0,63	0,63
4S-7LI45 ³	0,58	0,32	0,18	0,76	0,18	0,45	0,40
4S-4LI60 ³	0,74	0,32	0,22	0,76	0,22	0,67	0,60
4S-6LI60 ³	0,69	0,47	0,47	1,10	0,47	0,86	0,86
2S-4LV ⁴	0,58	0,34	0,15	0,81	0,36	0,28	0,16
2S-7LV ⁴	0,77	0,39	0,39	0,93	0,93	0,37	0,37
2S-10LV ⁴	0,72	0,18	0,18	0,44	0,44	0,36	0,31
2S-7LI45 ⁴	1,27	0,47	0,37	1,10	0,88	0,61	0,55
2S-10LI45 ⁴	1,07	0,55	0,35	1,30	0,84	0,57	0,47
2S-4LI60 ⁴	1,42	0,64	0,44	1,51	1,04	0,80	0,72
2S-6LI60 ⁴	1,04	0,47	0,47	1,11	1,11	0,80	0,80
2S-9LI60 ⁴	0,83	0,43	0,43	1,02	1,02	0,80	0,60
AV	0,90	0,43	0,32	1,01	0,70	0,64	0,56
SD	0,23	0,16	0,16	0,38	0,32	0,26	0,26
COV	0,26	0,38	0,50	0,38	0,45	0,40	0,47

AV – average value; SD – Standard deviation; COV - Coefficient of variety; ¹ by Kotynia (2007), ² by Dias & Barros (2008), ³ by Dias et. al (2007), ⁴ by Dias & Barros (2010)

Table 2. Comparison of test and calculated NSM FRP shear round bars contribution ratios

Beam	$V_{f,test} / V_{f,cal}$						
	<i>Adapted fib</i>	Modified Nanni et. al (2004)		Modified Bianco et. al (2009)			
	$\varepsilon_f=2,0\text{‰}$	$\varepsilon_f=5,9\text{‰}; \tau_b=16,1\text{MPa}$	$\varepsilon_f=4,0\text{‰}; \tau_b=6,81\text{MPa}$	min L_{tot}	max L_{tot}		
		min L_{tot}	max L_{tot}	min L_{tot}	max L_{tot}		
B90-7 ⁵	0,46	0,34	0,15	0,81	0,34	0,39	0,23
B90-5 ⁵	0,50	0,22	0,22	0,52	0,52	0,44	0,44
B45-7 ⁵	0,99	0,47	0,29	1,12	0,69	0,95	0,61
B45-5 ⁵	0,82	0,48	0,48	1,13	1,13	0,78	0,78
AV	0,69	0,38	0,29	0,90	0,67	0,61	0,52
SD	0,22	0,11	0,12	0,25	0,29	0,23	0,20
COV	0,32	0,28	0,43	0,28	0,44	0,36	0,40

⁵ by De Lorenzis & Nanni (2001)

The Nanni et. al formula predicts the NSM shear contribution $V_{f,test} / V_{f,cal}$ with the average value of 1,01 and 0,9 for the strips and round bars, respectively. The adapted fib formula gives predicted average $V_{f,test} / V_{f,cal}$ values of 0,90 and 0,69 for the strips and bars, respectively. The lowest average $V_{f,test} / V_{f,cal}$ values of 0,64 and 0,61, calculated based on the modified Bianco et. al model is effected by the overestimated average semi-cone surface cut by the diagonal shear

crack. The failure modes observed in the tests indicated that the NSM strips/bars debond with detached concrete cover from the concrete core in the plane of the FRPs depth. It seems that even the generatrix is inclined to the NSM axis at β angle in longitudinal beam's direction, it does not exceed the concrete depth in the transversal beam's cross section. This opinion suggests the author to change the semi-cone shape to the semi-ellipse with the minor axis length lower than the concrete cover or to the semi-pyramid with the height of the support plane lower than the concrete cover. The comparative study of this approach is in author's preparation.

Moreover, as the spacing between subsequent NSM stirrups is reduced, their semi-conical fracture surfaces overlap resulting in progressive decrease in the envelope area, which was confirmed in the published shear tests. The beam's failure was characterized by the two-side debonding of a group NSM strips/bars, together with detached lateral concrete cover, from the core of the beam. Such a mode of failure indicated a negative influence of the NSM spacing reduction on the shear strength. This local horizontal tensile stress component occurrence perpendicular to the beam's web proves the group NSM debonding with the concrete cover above and below the diagonal shear crack. The NSM strip interaction should be considered in the design recommendation of the minimum FRP spacing along the longitudinal beam's axis or the additional anchors are needed to avoid a group NSM detachment from the beam's core.

3 CONCLUSIONS

Three formulas of the NSM FRP shear contribution to the shear strength of the T cross-section RC beams were used for analysis of the test results. The Nanni's et. al approach gives the most satisfied predictions. The versatile model by Bianco et. al considers two main failure approaches: FRP debonding and the concrete tensile fracture. Although the model corresponds to the real concrete fracture observed in the tests, it overestimates the semi-cone surface of the fracture plane. This problem needs more experimental and calculated work to justify the underlined issues in aspect of the following variable parameters: steel transversal interaction, the concrete strength, the minimal FRP spacing and the additional anchorage of the NSM reinforcement in order to avoid the concrete cover detachment.

References

- Bianco, V, Barros JAO. and Monti. 2009. Three dimensional mechanical model for simulating the NSM FRP strips shear strength contribution to RC beams. *Engineering Structures*, 31:815-826.
- De Lorenzis, L. and Nanni, A. 2001. Shear Strengthening of Reinforced Concrete Beams with Near-Surface Mounted Fiber-Reinforced Polymer Rods. *ACI Structural Journal*, 98(1): 60-68.
- De Lorenzis, L. 2002. Strengthening of RC Structures with Near-Surface Mounted FRP rods. Università Degli Studi di Lecce, Italy. PhD Thesis.
- Dias, SJE. and Barros, JAO. 2008. Shear strengthening of T cross section reinforced concrete beams by near surface mounted technique. *Journal of Composites for Construction*, 12(3): 300-311.
- Dias, SJE. and Barros, JAO. 2010. Performance of reinforced concrete t beams strengthened in shear with NSM CFRP. *Engineering Structures*, 32: 373-384.
- Dias, SJE, Bianco, V, Barros JAO. and Monti G. 2007. Low strength T-cross section RC beams shear-strengthened by NSM technique, Proc. Materiali ed Approcci Innovativi per il Progetto in Zona Sismica e la Mitigazione della Vulnerabilità delle Strutture, Salerno, CD ROM.
- fib - Bulletin 14, 2001. Externally bonded FRP reinforcement for RC structures, technical report by Task Group 9.3 FRP reinforcement for concrete structures, *fib*, July, 130 pp.
- Kotynia, R. 2007. Shear strengthening of RC beams with NSM CFRP laminates. Proc. FRPRCS-8, Patras, Greece, CD ROM.
- Nanni, A, Di Ludovico, M, and Parretti, R. 2004. Shear strengthening of a PC bridge girder with NSM CFRP rectangular bars. *Advances in Structural Engineering*, 7, N° 4: 97-109.